Available online at www.sciencedirect.com
SCIENCE DIRECT®
Journal of Sound and Vibration 276 (2004) 81–103
JOURNAL OF SOUND AND VIBRATION
www.elsevier.com/locate/jsvi

A comparison of shortening of the projection to axial elasticity

V. Radisavljevic, H. Baruh*

Department of Mechanical and Aerospace Engineering, Rutgers University, 98 Brett Road, Piscataway, NJ 08854-8058, USA

Received 31 July 2001; accepted 20 July 2003

Abstract

In this paper we consider the combined bending and axial vibration of beams and we analyze the magnitudes of the different effects that contribute to the motion. Specifically, we consider the transverse elasticity, the axial elasticity, and the shortening of the projection. The goal of our study is to ascertain the circumstances under which the axial elasticity is larger than the shortening of the projection and vice versa. We show that for the majority of cases the shortening of the projection has larger amplitude than the axial stretch. We also develop a general closed-form solution for the response when a force is applied at a free end.

1. Introduction

An important issue when modelling beams and beam-like structures is to whether include the axial deformation in the mathematical model. For a beam, such deformation is due to two primary sources: (1) The axial elasticity, and (2) the shortening of the projection due to curvature of the elastic axis. In general, the presence of axial forces dictates whether such effects need to be considered. For example, if there is a persistent axial force, such as a compressive force as in the case of a column, or a continuous tensile force, as in the case of a rotating beam, the shortening of the projection must be included in the mathematical model [1].

In the absence of a persistent external force in the axial direction, conventional wisdom has dictated to include the axial elasticity in the mathematical model, before including the shortening of the projection. Part of the reason for this is the non-linearity of the expression describing the shortening of the projection. Also, when viewed from the definition of axial strain, the contribution of axial elasticity is a first order term, while the shortening of the projection is a second order term.

*Corresponding author. Tel.: +1-732-445-3680; Fax: +1-732-445-3124.
E-mail address: baruh@jove.rutgers.edu (H. Baruh).

0022-460X/$ - see front matter
doi:10.1016/j.jsv.2003.07.013

In this paper, we study the magnitude of the shortening of the projection and the axial stretch for the vibration of beams. We show that the axial elasticity and the shortening of the projection in most cases have comparable magnitudes and we develop a ratio of the maximum values of these quantities. We demonstrate that in the majority of cases the shortening of the projection has a more significant contribution. The analysis lead to guidelines that one can follow when selecting the mathematical model of a slender beam.

2. Kinematic equation

We consider a slender beam, that is, whose length is considerably larger than its cross-sectional dimensions, such as the beam in Fig. 1.

We consider small deformations and assume that shear deformation can be ignored. We further ignore the coupling between bending and torsion. It then becomes possible to only consider the stress in the x direction. We will model the combined bending and axial motion. Fig. 2 shows the deformed beam axis, where point A on the beam axis has moved to A^*.

In this configuration, s denotes the distance traversed along the beam axis from $x = 0$ to the deformed position A^*, with u, v and w denoting the components of the deformation along the x, y and z axes. The deformation of a point x on the beam axis is described by

$$\mathbf{r}(x,t) = (x + u(x,t))\mathbf{i} + v(x,t)\mathbf{j} + w(x,t)\mathbf{k} \tag{1}$$

and we also assume that the section rotations of the beam in the y and z directions are approximated by

$$\theta_y(x,t) = -\frac{\partial w(x,y)}{\partial x} = -w'(x,t), \quad \theta_z(x,t) = \frac{\partial v(x,y)}{\partial x} = v'(x,t), \tag{2}$$

where θ_y and θ_z are the components of the second rotation. Hence, the slope of the beam, denoted by $\theta(x,t)$, can be expressed as

$$\theta(x,t) = \sqrt{v'^2(x,t) + w'^2(x,t)}. \tag{3}$$

The distance traversed along the beam axis $s(x,t)$ is

$$s(x,t) = x + e(x,t), \tag{4}$$

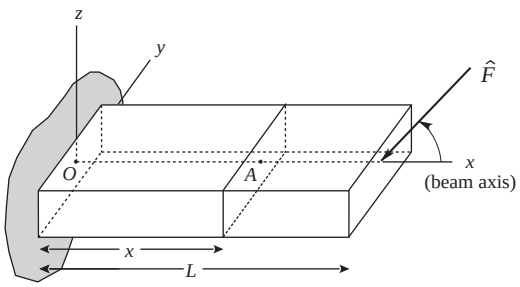

Fig. 1. The beam.

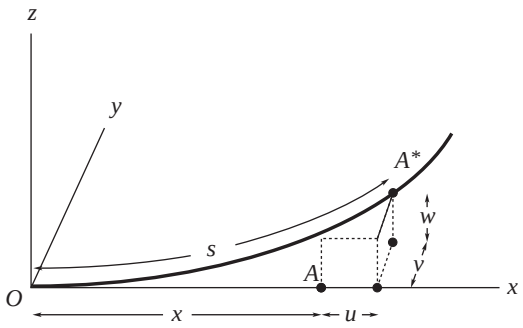

Fig. 2. The deformed beam axis.

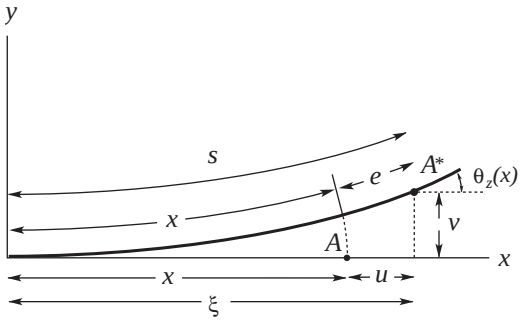

Fig. 3. Projection onto beam axis.

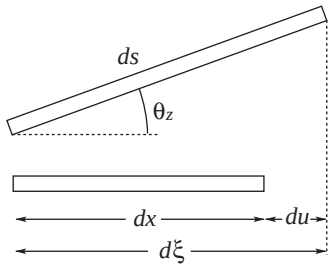

Fig. 4. A differential element.

in which $e(x,t)$ is the elastic stretch, due to the axial elasticity. We next consider the projection of the deformed point A^* onto the beam axis. The configuration is shown in Figs. 3 and 4, the latter showing a differential element.

We denote the length of the projection by $\xi(x,t)$ so that $\xi(x,t) = x + u(x,t)$. Using a Taylor series expansion of Eq. (3), the projection of the differential element $\mathrm{d}s$ onto the x-axis can be expressed as

$$\mathrm{d}\xi(x,t) \approx \mathrm{d}s\left(1 - \tfrac{1}{2}\theta^2(x,t)\right) = \mathrm{d}s - \tfrac{1}{2}(v'^2(x,t) + w'^2(x,t)) \tag{5}$$

which when integrated gives

$$\xi(x,t) = x + u(x,t) \approx s(x,t) - \frac{1}{2}\int_0^{s(x,t)} \left[\left(\frac{\partial v}{\partial \sigma}\right)^2 + \left(\frac{\partial w}{\partial \sigma}\right)^2\right] \mathrm{d}\sigma. \tag{6}$$

Considering that e and u are small compared to s and x, we approximate the upper limit in the above equation by x, which yields

$$u(x,t) = e(x,t) - \frac{1}{2}\int_0^{x} \left[\left(\frac{\partial v}{\partial \sigma}\right)^2 + \left(\frac{\partial w}{\partial \sigma}\right)^2\right] \mathrm{d}\sigma. \tag{7}$$

This relation can also be obtained by considering the non-linear strain–displacement relationships. Indeed, writing

$$\varepsilon_{xx} = \frac{\partial u}{\partial x} + \frac{1}{2}\left[\left(\frac{\partial u}{\partial x}\right)^2 + \left(\frac{\partial v}{\partial x}\right)^2 + \left(\frac{\partial w}{\partial x}\right)^2\right] + h.o.t. \tag{8}$$

and ignoring the $(\partial u/\partial x)^2$ term and integrating, we obtain Eq. (7). Also, the above equation can be written as

$$\varepsilon_{xx}(x,t) = e'(x,t). \tag{9}$$

Let us go back to Eq. (7). We observe that the deformation in the x direction, $u(x,t)$, has two components. The first, $e(x,t)$, is due to the axial elasticity, and the second, denoted by $S(x,t)$ and equal to $-\frac{1}{2}\int_0^x [(\partial v/\partial\sigma)^2 + (\partial w/\partial\sigma)^2]\,\mathrm{d}\sigma$, is due to the shortening of the projection. The word *shortening* is associated with the observation that this term is always negative.

The issue we investigate next is the magnitude of these two contributions along the x-axis. Traditionally, one assumes that the stretch has a larger value because it is a first order term and the shortening is of second order. To analyze this issue in more detail, we will derive the equations of motion and obtain the response.

3. Equations of motion

We will obtain the equations of motion using Hamilton's equations. One can use two sets of variables to derive the equations of motion: e, v, w or u, v, w. It turns out that it is more convenient to write the kinetic energy in terms of u, v, w and the potential energy in terms of e, v, w. A comprehensive survey of different approaches to model the shortening of the projection and its application to rotating beams can be found in Ref. [2]. We write the energy terms as

$$2T(t) = \int_0^L \mu(x)(\dot{\mathbf{r}}(x,t)\cdot\dot{\mathbf{r}}(x,t))\,\mathrm{d}x = \int_0^L \mu(x)(\dot{u}^2(x,t) + \dot{v}^2(x,t) + \dot{w}^2(x,t))\,\mathrm{d}x, \tag{10}$$

$$2V(t) = \int_0^L (EA(x)[e'(x,t)]^2 + EI_{zz}(x)[v''(x,t)]^2 + EI_{yy}(x)[w''(x,t)]^2)\,\mathrm{d}x, \tag{11}$$

in which $\mu(x)$ is the mass unit per unit length, $\mu(x) = \rho A(x)$ with $A(x)$ denoting the cross-section area and ρ is the density.

Let us begin with u, v, w. We write the virtual work as

$$\delta W = \int (p_x(x,t)\delta u + p_y(x,t)\delta v + p_z(x,t)\delta w)\,\mathrm{d}x, \tag{12}$$

where p_x, p_y, p_z are the components of the force along the xyz axes. We invoke Hamilton's Principle and carry out the details of the integration by parts. Introducing the quantity $P(x,t)$, defined as

$$P(x,t) = EA(x)e'(x,t) = EA(x)u'(x,t) + \tfrac{1}{2}EA(x)\left[\left(\frac{\partial v}{\partial x}\right)^2 + \left(\frac{\partial w}{\partial x}\right)^2\right], \tag{13}$$

in which $P(x,t)$ describes the internal force about the elastic axis; we obtain the equations of motion as

$$\mu(x)\ddot{u}(x,t) - \frac{\partial}{\partial x}P(x,t) = p_x(x,t), \tag{14}$$

$$\mu(x)\ddot{v}(x,t) + \frac{\partial^2}{\partial x^2}\left[EI_z(x)\frac{\partial^2 v(x,t)}{\partial x^2}\right] - \frac{\partial}{\partial x}\left[P(x,t)\frac{\partial v(x,t)}{\partial x}\right] = p_y(x,t), \tag{15}$$

$$\mu(x)\ddot{w}(x,t) + \frac{\partial^2}{\partial x^2}\left[EI_y(x)\frac{\partial^2 w(x,t)}{\partial x^2}\right] - \frac{\partial}{\partial x}\left[P(x,t)\frac{\partial w(x,t)}{\partial x}\right] = p_z(x,t). \tag{16}$$

These equations are non-linear due to the coupling between the axial and transverse motions.

Let us next consider the motion description in terms of e, v, w. Here, we retain the same form of the potential energy, but rewrite the velocity of the differential element at x as

$$\dot{\mathbf{r}}(x,t) = \dot{e}(x,t)\mathbf{i}' + \dot{v}(x,t)\mathbf{j} + \dot{w}(x,t)\mathbf{k} \tag{17}$$

in which $\mathbf{i}'(x,t)$ is the unit vector along the deformed elastic axis. In essence, we are writing the velocity in terms of a set of normal–tangential co-ordinates. The vector $\mathbf{i}'$ denotes the tangential direction with v and w denoting the location of point x. It follows that the kinetic energy has the form

$$2T(t) = \int_0^L \mu(\dot{e}^2 + \dot{v}^2 + \dot{w}^2 + 2\dot{e}(\dot{v}\sin\theta_z - \dot{w}\sin\theta_y))\,\mathrm{d}x. \tag{18}$$

Application of Hamilton's principle leads to a set of non-linear equations of motion. Our goal here is to compare the magnitudes of the elastic deformation $e(x,t)$ and shortening of the projection $S(x,t)$ in closed form. To this end, we consider the expression for the kinetic energy in the above equation and neglect all terms that are higher order than quadratic, namely those that involve $\sin\theta$. We justify this assumption by noting that θ_y and θ_z are small quantities. As a result, the kinetic energy reduces to

$$2T(t) \approx \int_0^L \mu(\dot{e}^2(x,t) + \dot{v}^2(x,t) + \dot{w}^2(x,t))\,\mathrm{d}x. \tag{19}$$

This approximation can also be obtained from Eqs. (7) and (10) if we consider that the time rate of change of the shortening of the projection is small, so that it can be neglected.

We write the virtual work in terms of the components of the external forces along the x', y, z axes in the form

$$\delta W = \int (p_{x'}(x,t)\delta e + p_y(x,t)\delta v + p_z(x,t)\delta w)\,\mathrm{d}x \tag{20}$$

in which $p_{x'}$, p_y, p_z are the components of the axial force along the $x'yz$ axes. Considering a uniform cross-section and carrying out the algebra, we obtain the linearized equations of motion in the form

$$\mu\ddot{e}(x,t) - EAe''(x,t) = p_{x'}(x,t), \tag{21}$$

$$\mu\ddot{v}(x,t) + EI_z v''''(x,t) = p_y(x,t), \tag{22}$$

$$\mu\ddot{w}(x,t) + EI_y w''''(x,t) = p_z(x,t), \tag{23}$$

subject to the appropriate boundary conditions. These represent three independent linear equations that are about a set of non-orthogonal axes. By contrast, had we used u, v, w as variables, the relationship between u, e, v, and w would be harder to compare. Also, Refs. [2,3] indicate that especially when a discretized solution is to be used, selecting e, v, w is more desirable, as a substantial component of $u(x,t)$ is the shortening of the projection.

To compare the magnitudes of $u(x,t)$, $e(x,t)$ and the shortening of the projection $S(x,t)$, we recognize three types of models: (1) the "exact" model, which includes both the elastic stretch and shortening of the projection; (2) the approximate model, including the elastic stretch but not the shortening of the projection; and (3) the approximate model, including shortening of the projection but not the elastic stretch.

The question then becomes which of the two approximate models is more accurate. Traditionally, and in the absence of a persistent axial force, model (2) has been used more frequently. To answer our question, one can simulate the equations of motion and compare the values of u, e, and S. Before we do that, we will first obtain a closed-form approximation to the response of the linearized system.

4. Non-dimensionalization and response

We begin with non-dimensionalizing the problem. Consider Eqs. (21)–(23) and rewrite them as

$$\mu^*\ddot{e}^*(x^*,t^*) - E^*A^*e^{*\prime\prime}(x^*,t^*) = p^*_{x^*}(x^*,t^*), \tag{24}$$

$$\mu^*\ddot{v}^*(x^*,t^*) + E^*I^*_{z^*}v^{*\prime\prime\prime\prime}(x^*,t^*) = p^*_{y^*}(x^*,t^*), \tag{25}$$

$$\mu^*\ddot{w}^*(x^*,t^*) + E^*I^*_{y^*}w^{*\prime\prime\prime\prime}(x^*,t^*) = p^*_{z^*}(x^*,t^*), \tag{26}$$

in which the starred quantities are variables with dimensions. The beam is of length L^*. We will use the non-dimensionalization procedure in Ref. [4]. We simplify, without loss of generality, by neglecting the transverse motion in the z direction. The area moment of inertia about the z-axis and mass per unit length are written in terms of the cross-sectional area as

$$I^*_{z^*} = A^*\kappa^{*2}, \quad \mu^* = A^*\rho^*, \tag{27}$$

where A^* is the cross-sectional area, κ^* is the radius of gyration and ρ^* is the density. We introduce the quantities

$$L = \frac{L^*}{L^*}, \quad x = \frac{x^*}{L^*}, \quad \mathrm{d}x = \frac{\mathrm{d}x^*}{L^*}, \quad e = \frac{e^*}{L^*}, \quad v = \frac{v^*}{L^*} \tag{28}$$

in view of which the partial derivatives have the form

$$\frac{\partial}{\partial x^{*k}} = \frac{1}{L^{*k}} \frac{\partial}{\partial x^k}. \tag{29}$$

We also have

$$A = \frac{A^*}{L^{*2}}, \quad t = t^* \varpi_1^*, \quad \rho = \rho^* \frac{L^{*6} \varpi_1^{*2}}{E^* I^*}, \tag{30}$$

where ϖ_1^* is the first natural frequency in bending, to be determined. Introducing all these substitutions to the equations of motion, we obtain the non-dimensionalized equations

$$\rho A \ddot{e}(x,t) - \frac{e''(x,t)}{\kappa^2} = p_x(x,t), \tag{31}$$

$$\rho A \ddot{v}(x,t) + v''''(x,t) = p_y(x,t), \tag{32}$$

in which $\kappa = \kappa^*/L^*$ is the non-dimensionalized radius of gyration and the forcing terms on the right-hand side are obtained by multiplying the starred quantities by $L^{*3}/E^* I^*$. Hence, we have reduced the number of non-dimensional parameters that govern the behavior of the axial and transverse motion to two, ρA and κ.

Next, consider the external excitation to be used in our comparison. We select a fixed–free bar and an excitation in the form of an impulsive force $\hat{F}$ applied at the tip of the bar. The impulsive force makes an angle of β with the x-axis. In terms of non-dimensional quantities, one can write this force as

$$p_y(x,t) = \hat{F}\delta(x-1)\delta(t)\sin\beta, \quad p_x(x,t) = \hat{F}\delta(x-1)\delta(t)\cos\beta. \tag{33}$$

Note that if a force is applied at a free end, the boundary conditions at that end change and the eigensolution of the fixed–free bar (bending or axial) cannot be used [5,6]. In Appendix A, we show a way of calculating a closed-form solution for the response due to a force applied at the free end of a beam. An alternative, which leads to the same result, is to think of the applied force acting on a point infinitesimally away from the free end ($\delta(x-1^-)$) and use this expression instead of ($\delta(x-1)$) in the above equation.

We now consider the eigensolution. For both the transverse and axial vibrations there is a closed-form solution. Using the expansions

$$v(x,t) = V(x)\mathrm{e}^{\mathrm{i}\varpi t}, \quad e(x,t) = E(x)\mathrm{e}^{\mathrm{i}\Omega t} \tag{34}$$

and defining the quantities $a^4 = \rho A \varpi^2$ and $b^2 = \rho A \kappa^2 \Omega^2$, we obtain the closed-form solutions to the corresponding characteristic equations as

$$a_1 = 1.875, \quad a_2 = 4.694, \quad a_3 = 7.855, \ldots; \quad b_1 = \pi/2, \quad b_2 = 3\pi/2, \quad b_3 = 5\pi/2. \tag{35}$$

Combining the above relations, we can obtain a relationship between the ratios of the first natural frequencies of the transverse and elastic motion as

$$\frac{\varpi_1}{\Omega_1} = \frac{a_1^2}{b_1}\kappa = 2.238\kappa. \tag{36}$$

The question then arises as to what a reasonable value for κ is. For a circular cross-section $A = \pi r^2$, $I = \pi r^4/4$, so that considering a slenderness ratio of $L/r = 10$ we obtain $\kappa = 1/20$. For a rectangular cross-section of b by $b/2$, taking a slenderness ratio of $b/L = 0.1$, we obtain that $\kappa \approx 1/65$. Actually, κ has its highest value for circular cross-sections. So, if we conservatively take $\kappa = 1/22.38$, then from the above equation we obtain

$$\frac{\varpi_1}{\Omega_1} = \frac{a_1^2}{b_1}\kappa = 2.238\kappa = 0.1. \tag{37}$$

Next we compare the amplitudes of the modes of vibration. We assume that the first mode dominates the motion, so that we will use a one mode expansion. Note that an impulsive force at a point $x = P$ has the effect of an initial velocity on each mode of magnitude $\phi_r(P)\hat{F}\sin\beta$ ($r = 1, 2, \ldots$), for the transverse motion and $\psi_r(P)\hat{F}\sin\beta$ for the axial deformation. A force applied at a free end changes the boundary conditions at that end, so one may raise the question of whether the eigenfunctions of the fixed–free beam can be used to obtain the solution. The general formulation for such a problem is studied in Refs. [5,6]. We show in Appendix A that the expression for the displacement and slope at the free end $x = 1$ due to a force applied at the end has the same form as when it is calculated for a force in the interior of the beam. The difference in the solutions is in the internal force and moment. Hence, for the transverse motion, the response of each mode to an impulsive force at $x = 1$ is

$$\eta_r(t) = \phi_r(1)\hat{F}\sin\beta\frac{\sin(\varpi_r t)}{\varpi_r}, \quad r = 1, 2, \ldots, \tag{38}$$

where $\phi_r(x)$ is the rth eigenfunction. This eigenfunction is normalized with respect to the mass using the relation

$$\int_0^1 \rho A\phi_1^2(x)\,\mathrm{d}x = 1. \tag{39}$$

It follows that the one mode approximation to the maximum amplitude of the tip of the beam has the form

$$v_{max} \approx \phi_1(1)\eta_1(t)_{max} = \frac{\phi_1^2(1)\hat{F}\sin\beta}{\varpi_1}. \tag{40}$$

In a similar fashion, we obtain the one mode approximation to the maximum value of the axial deformation

$$e_{max} \approx \psi_1(1)\eta_1(t)_{max} = \frac{\psi_1^2(1)\hat{F}\cos\beta}{\Omega_1}. \tag{41}$$

We next compare these maximum amplitudes. For the axial motion, the normalized eigenfunctions have the closed-form

$$\psi_r(x) = \sqrt{\frac{2}{\rho A}} \sin\left(\frac{(2r-1)\pi x}{2}\right), \quad r = 1, 2, \ldots. \tag{42}$$

Evaluating the first eigenfunction at $x = 1$ and introducing it to the above equation we obtain

$$e_{max} = \frac{2\hat{F}\cos\beta}{\Omega_1 \rho A}. \tag{43}$$

For the transverse motion, the first eigenfunction can be shown to be

$$\phi_1(x) = C_1\{(\sin(a_1 x) - \sinh(a_1 x)) - 1.362(\cos(a_1 x) - \cosh(a_1 x))\} \tag{44}$$

and using the value for a_1 from Eq. (35) we obtain

$$C_1 = \frac{1}{1.362\sqrt{\rho A}}. \tag{45}$$

Evaluating $\phi_1(x)$ at $x = 1$ we have $\phi_1(1) = 2.725C_1$, so that

$$\phi_1(1) = \frac{2.725}{1.362}\frac{1}{\sqrt{\rho A}} \approx \frac{2}{\sqrt{\rho A}}. \tag{46}$$

Introduction of this value into Eq. (40) gives

$$v_{max} = \frac{4\hat{F}\sin\beta}{\rho A \varpi_1}. \tag{47}$$

We are now ready to compare the maximum amplitudes of the transverse and elastic motions at the tip of the beam. Dividing Eq. (43) with Eq. (47) and using Eq. (36) we obtain

$$\frac{e_{max}}{v_{max}} = \frac{\varpi_1}{2\Omega_1 \tan\beta} = 1.119\frac{\kappa}{\tan\beta}. \tag{48}$$

Table 1 compares the amplitude ratio as a function of varying values for κ and β. In the majority of cases, the amplitude ratio is less than 1/20. This result should be considered in light of the fact that in the presence of elastic deformation in the z direction the curvature will be even larger, making e_{max}/v_{max} smaller than the estimate above. Also, it should be noted that in our previous estimate of κ we used a slenderness ratio of 10, so that for a longer beam, the amplitude ratio will be smaller.

Next, we calculate the maximum amplitude of the shortening of the projection at the tip of the beam. We employ the same one mode approximation and using Eq. (38) write the transverse displacement as

$$v(x,t) \approx \phi_1(x)\eta_1(t) = \phi_1(x)\phi_1(1)\hat{F}\sin\beta\frac{\sin(\varpi_1 t)}{\varpi_1} \tag{49}$$

Table 1
Amplitude ratio e_{max}/v_{max}

β (deg)	κ				
	1/20	1/30	1/40	1/50	1/60
10	0.3173	0.2115	0.1587	0.1269	0.1058
20	0.1537	0.1025	0.0769	0.0615	0.0512
30	0.0969	0.0646	0.0485	0.0388	0.0323
40	0.0667	0.0445	0.0333	0.0267	0.0222
50	0.0469	0.0313	0.0235	0.0188	0.0156
60	0.0323	0.0215	0.0162	0.0129	0.0108
70	0.0204	0.0136	0.0102	0.0081	0.0068
80	0.0099	0.0066	0.0049	0.0039	0.0033

so that

$$S(1,t) = -\frac{1}{2}\int_0^1 v'^2(x,t)\,\mathrm{d}x = -\frac{1}{2}\frac{\phi_1^2(1)}{\varpi_1^2}\hat{F}^2\sin^2\beta\sin^2(\varpi_1 t)\int_0^1 {\phi_1}'^2(x)\,\mathrm{d}x. \tag{50}$$

Introducing the definition of the first eigenfunction from Eq. (44) and the value of C_1 from Eq. (45) we obtain

$$\int_0^1 {\phi_1}'^2(x)\,\mathrm{d}x = 8.625C_1 = \frac{4.648}{\rho A}. \tag{51}$$

Recalling that $\varpi_1 = a_1^2/\sqrt{\rho A} = 1.875^2\sqrt{\rho A}$ and $\phi_1(1) = 2/\sqrt{\rho A}$, the maximum value of the shortening of the projection at the tip of the beam becomes

$$S_{max} = -2.324\frac{\phi_1^2(1)}{\varpi_1^2}\hat{F}^2\sin^2\beta = -0.7521\frac{\hat{F}^2\sin^2\beta}{\rho A}. \tag{52}$$

We next calculate the amplitude ratio of the shortening of the projection to the transverse displacement. Dividing Eq. (52) by Eq. (47) we obtain

$$\frac{S_{max}}{v_{max}} = 0.6610\frac{\hat{F}}{\sqrt{\rho A}}\sin\beta. \tag{53}$$

Hence, the magnitude of the amplitude ratio is governed by the ratio of the applied impulsive force to the square root of the mass density. To determine a realistic value for the ratio, we go back to Eq. (47), so that

$$v_{max} = \frac{4\hat{F}\sin\beta}{\rho A\varpi_1} = \frac{4}{1.875^2}\frac{\hat{F}\sin\beta}{\sqrt{\rho A}} = 1.138\frac{\hat{F}\sin\beta}{\sqrt{\rho A}}. \tag{54}$$

Introducing this expression into the ratio in Eq. (53), we obtain

$$\frac{S_{max}}{v_{max}} = \frac{0.6610}{1.138}v_{max} = 0.5808v_{max}. \tag{55}$$

Table 2
Amplitude ratio S_{max}/e_{max}

β (deg)	κ				
	1/20	1/30	1/40	1/50	1/60
10	0.0921	0.1382	0.1843	0.2303	0.2764
20	0.1902	0.2853	0.3803	0.4754	0.5705
30	0.3017	0.4525	0.6033	0.7542	0.9050
40	0.4384	0.6576	0.8769	1.0961	1.3153
50	0.6227	0.9340	1.2454	1.5567	1.8681
60	0.9050	1.3575	1.8100	2.2625	2.7150
70	1.4356	2.1533	2.8711	3.5889	4.3067
80	2.9632	4.4449	5.9265	7.4081	8.8897

A reasonable value for v_{max} is 0.05 (we assume the tip of the beam deforms by a ratio of 1/20 of its length), which gives

$$\frac{S_{max}}{v_{max}} = -0.05 * 0.5808 = 0.0290. \tag{56}$$

We next compare the amplitude ratio of the shortening of the projection and the axial deformation. Dividing Eq. (55) by Eq. (48) gives

$$\frac{S_{max}}{e_{max}} = \frac{0.5808}{1.119}\frac{v_{max}\tan\beta}{\kappa} = 0.5255\frac{v_{max}\tan\beta}{\kappa}. \tag{57}$$

Table 2 compares this ratio for varying values of the radius of gyration κ, angle β and $v_{max} = 0.05$. As can be seen, in the majority of cases the shortening of the projection has a larger magnitude than the axial deformation. This indicates that when including axial deformation effects in the mathematical model, one should check the beam parameters and the applied load, so as to determine whether the shortening of the projection should be included before the axial elasticity.

5. Multi-mode analysis

The results of the previous section were based on a single mode approximation of the response. In this section, we consider a multi-mode expansion of both the axial and transverse deformation and we compare the amplitude ratios as well as responses. In our expansion of the axial deformation, we use (m modes) twice as many modes as we do for the transverse deformation (n modes). This is because the eigenvalues of the axial deformation increase in arithmetic progression and the eigenvalues of the transverse deformation increase in geometric progression, resulting in more modes participating in the motion for the axial deformation.

Complete derivations for the axial and transverse deformation and the shortening of the projection are presented in Appendix A. In this section we use the actual quantities for all variables, not the non-dimensionalized ones.

The impulsive forces acting at the end of the beam are related by

$$\hat{F}_e = \hat{F}\cos(\beta), \quad \hat{F}_v = \hat{F}\sin(\beta). \tag{58}$$

The maximum values for the transverse and elastic motion, and the shortening of the projection appear at the tip of the beam (i.e., $x = L$). Introducing a new function

$$f_{vn}(t) = \sum_{r=1}^{n} \frac{\bar{V}_r^2(L)}{b_r^2}\sin(\omega_r t) \leqslant \sum_{r=1}^{n} \frac{\bar{V}_r^2(L)}{b_r^2} = f_{vn\,max}, \quad n = 1, 2, 3, \ldots, \tag{59}$$

the maximum amplitude for the transverse vibration as function of number of modes used is

$$v^n(L,t) = \hat{F}\frac{1}{\mu L}\sqrt{\frac{\rho}{E\kappa^2}}\sin(\beta) f_{vn}(t) \leqslant v^n_{max} = \hat{F}\frac{1}{\mu L}\sqrt{\frac{\rho}{E\kappa^2}}\sin(\beta) f_{vn\,max}, \quad n = 1, 2, 3, \ldots. \tag{60}$$

The magnitude of the impulsive force can be expressed as a function of v^n_{max} as

$$\hat{F} = \frac{v^n_{max}\mu L}{\sin(\beta) f_{vn\,max}}\sqrt{\frac{E\kappa^2}{\rho}}, \quad n = 1, 2, 3, \ldots. \tag{61}$$

Therefore, the maximum amplitude for the shortening of the projection of the tip of the beam, as a function of number of modes used, is

$$S^n_{max} = -\frac{\hat{F}^2\sin^2(\beta)}{2}\frac{\rho}{E\kappa^2}\frac{1}{(\mu L)^2}\sum_{r=1}^{n}\sum_{s=1}^{n} s_{rs} = -\frac{v^{n^2}_{max}}{2f^2_{vn\,max}}\sum_{r=1}^{n}\sum_{s=1}^{n} s_{rs}, \tag{62}$$

where

$$s_{rs} = \frac{\bar{V}_r(L)}{b_r^2}\frac{\bar{V}_s(L)}{b_s^2}\int_0^L \frac{\mathrm{d}\bar{V}_r(x)}{\mathrm{d}x}\frac{\mathrm{d}\bar{V}_s(x)}{\mathrm{d}x}\mathrm{d}x. \tag{63}$$

Using the new expression for the impulsive force, we obtain the maximum amplitude for the axial stretch e^m_{max} as a function of the number of modes used at $x = L$ as

$$e^m(L,t) = \frac{2v^n_{max}\kappa}{\tan(\beta)} f_{em}(t) \leqslant e^m_{max} = \frac{v^n_{max} f_{em\,max}}{\tan(\beta) f_{vn\,max}} 2\kappa, \tag{64}$$

where

$$f_{em}(t) = \sum_{r=1}^{m}\frac{\bar{U}_r^2(L)}{a_r}\sin(\Omega_r t) \leqslant \sum_{r=1}^{m}\frac{\bar{U}_r^2(L)}{a_r} = f_{em\,max}, \quad m = 1, 2, 3, \ldots. \tag{65}$$

Finally, the amplitude ratio of the shortening of the projection and the axial stretch is given as

$$\frac{S^n_{max}}{e^m_{max}} = \frac{v^n_{max}\tan(\beta)}{4\kappa f_{vn\,max} f_{em\,max}}\sum_{r=1}^{n}\sum_{s=1}^{n} s_{rs}. \tag{66}$$

When we use only one mode for both axial and transverse deformation, then expressions for e^m_{max}, v^n_{max}, and S^n_{max} are exactly the same as ones derived in the previous section, which proves the validity of that analysis. Here, we examine the ratio S^n_{max}/e^m_{max} when axial and transverse deformations were calculated with more then one mode. Figs. 5–8 show the ratio S^n_{max}/e^m_{max} versus v^n_{max} for varying values of the radius of gyration. As can be expected, the results follow the trend of Table 2. The different lines on the plots correspond to values of the angle β in the range 10–70°,

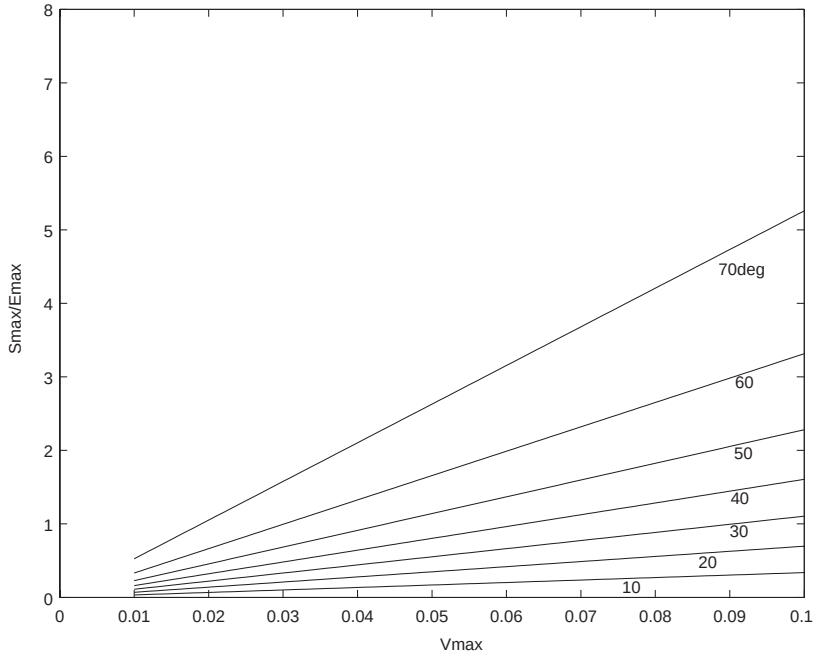

Fig. 5. S_{max}/e_{max} vs. v_{max} for $\kappa = 0.04$ and 2–4 modes in expansion.

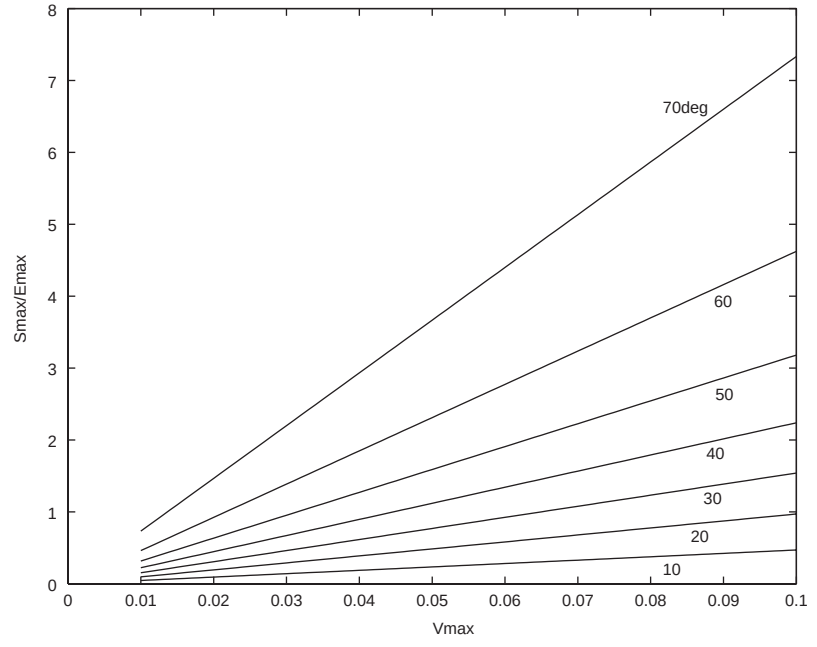

Fig. 6. S_{max}/e_{max} vs. v_{max} for $\kappa = 0.04$ and 4–8 modes in expansion.

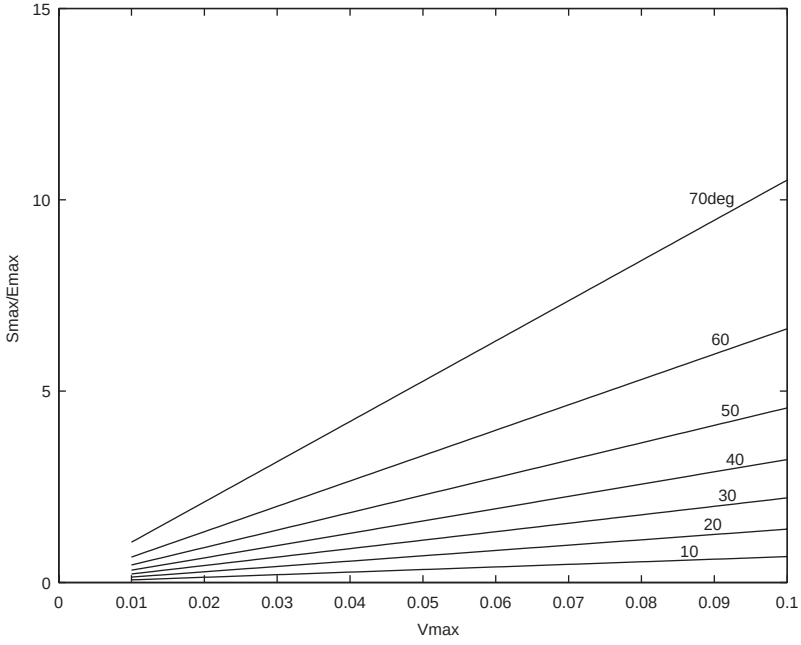

Fig. 7. S_{max}/e_{max} vs. v_{max} for $\kappa = 0.02$ and 2–4 modes in expansion.

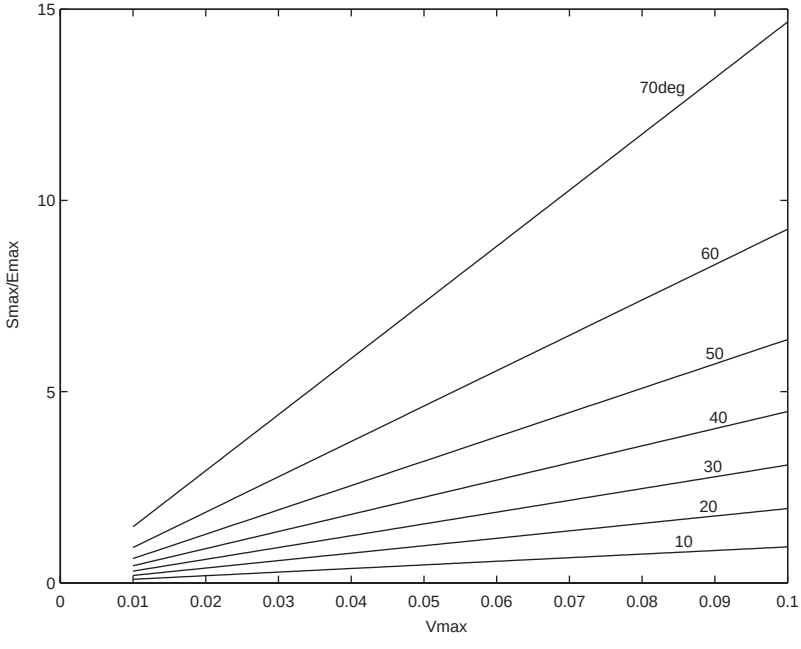

Fig. 8. S_{max}/e_{max} vs. v_{max} for $\kappa = 0.02$ and 4–8 modes in expansion.

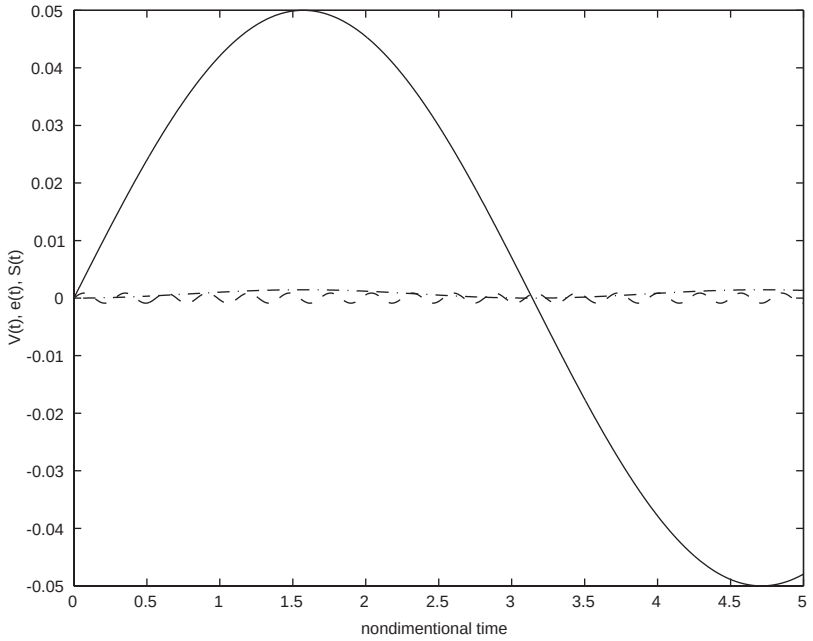

Fig. 9. Comparison of response for $\beta = 45^\circ$; —, $v(L,t)$; -- $e(L,t)$; $\cdot\text{-}\cdot$, $S(L,t)$.

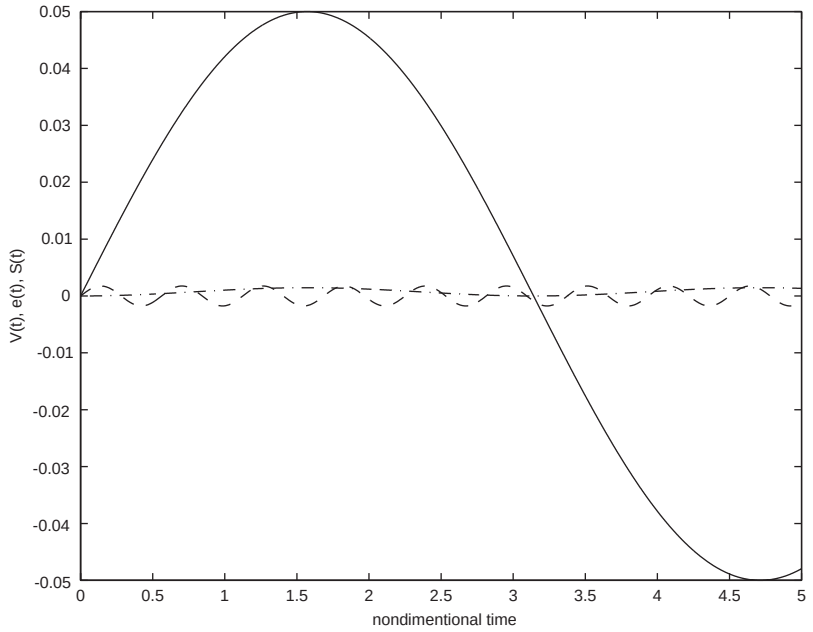

Fig. 10. Comparison of response for $\beta = 45^\circ$; —, $v(L,t)$; -- $e(L,t)$; $\cdot\text{-}\cdot$, $S(L,t)$.

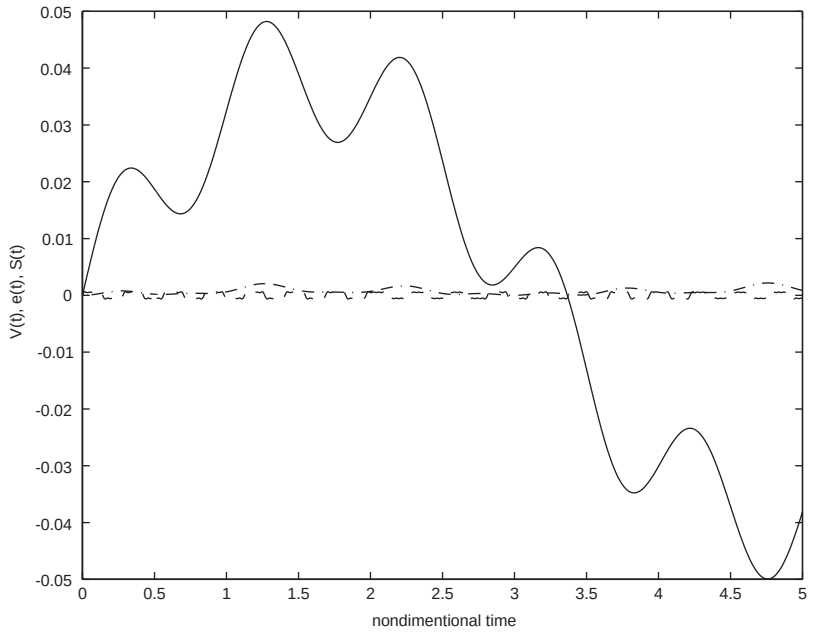

Fig. 11. Comparison of response for $\beta = 45^\circ$; —, $v(L,t)$; - - $e(L,t)$; $\cdots$, $S(L,t)$.

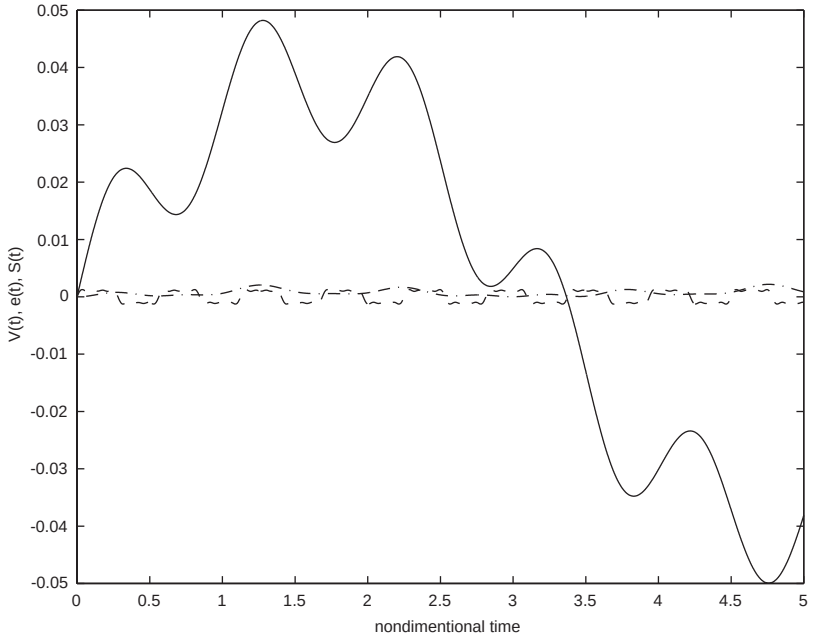

Fig. 12. Comparison of response for $\beta = 45^\circ$; —, $v(L,t)$; - - $e(L,t)$; $\cdots$, $S(L,t)$.

with increments of 10°. We observe that the ratio S^n_{max}/e^m_{max} grows slightly larger than the one mode estimate. Hence, the single mode approximation and Eq. (57) can be used as a guideline to determine whether the beam one considers needs to be modelled together with shortening or axial elasticity. When the results of the one mode analysis are inconclusive the multi-mode analysis may be required.

Next, we consider the simulation of the system response. We use the same conditions as in the previous section (no initial deformation or velocity, an impulsive force, with a variety of number modes for transverse (n) and the axial (m) deformation). The simulation results are shown in Figs. 9–12 for the tip of the beam for the cases of $\kappa = 0.02$ and $\kappa = 0.04$. The impulsive force $\hat{F}$ is selected using Eq. (61) so that the maximum amplitude of the transverse deformation is $v^n_{max} = 0.05$ m and $L = 1$ m.

We observe that the motion amplitudes are within the range predicted in the previous analysis, with the shortening of the projection assuming somewhat larger values. Hence, the guideline developed in Eq. (57) from a single mode analysis is a reliable measure to use in a multi-mode analysis. Furthermore, we see a slower time dependence of the shortening of the projection, thus justifying the assumptions made earlier that the shortening is a slowly varying term and that in most cases it can be treated as a quasi-static expression [3].

6. Response of non-linear model

In previous sections of this paper, we analyzed the response amplitudes of the axial and transverse motion. For the choice of the motion variables, the potential energy is quadratic and the kinetic energy contains terms higher than quadratic. The closed-form analysis and response of the previous sections was based on eliminating the higher order terms from the kinetic energy. The resulting equations of motion then became linear.

The question arises as to the effects of these non-linear terms. Let us examine the non-linear equations of motion when the higher order terms are included. Using the assumed modes method, we introduce the expansion of the response for the axial and transverse motions into the kinetic energy and invoke Langrange's equations, which result in a set of non-linear equations.

Encouraged by the results of the previous sections, where a single mode analysis accurately predicts the overall response, we will again consider a one mode expansion of the axial and transverse motions. We further simplify the problem by considering transverse deformation in the y direction only, setting $w(x,t) = 0$. In addition, we simplify $\sin(\theta_z) \approx v'(x,t)$. Using the starred notation, which indicates that the quantities we are using have dimensions, the kinetic and potential energies have the form

$$2T^* = \int_0^{L^*} \mu^*(\dot{e}^{*2}(x^*,t^*) + \dot{v}^{*2}(x^*,t^*) + 2\dot{e}^*(x^*,t^*)\dot{v}^*(x^*,t^*)v'^*(x^*,t^*))\,\mathrm{d}x^*, \tag{67}$$

$$2V^*(t) = \int_0^{L} (E^*A^*(x^*)[e'^*(x^*,t^*)]^2 + E^*I^*_{z^*z^*}(x^*)[v''^*(x^*,t^*)]^2)\,\mathrm{d}x^*. \tag{68}$$

Before invoking the assumed modes, it is helpful to non-dimensionalize the energy terms. Recalling that $\int_0^{L^*} \mathrm{d}x^* = L^* \int_0^1 \mathrm{d}x$ and dividing the kinetic and potential energies by E^*L^{*3} we

obtain

$$2T = A\rho \int_0^1 (\dot{e}^2(x,t) + \dot{v}^2(x,t) + 2\dot{e}(x,t)\dot{v}(x,t)v'(x,t))\,\mathrm{d}x, \tag{69}$$

$$2V = \int_0^1 \left(\frac{e'(x,t)^2}{\kappa^2} + (v''(x,t)^2)\right)\mathrm{d}x. \tag{70}$$

We write the elastic motion using a one term expansion as

$$e(x,t) = \psi(x)\eta(t), \quad v(x,t) = \phi(x)z(t), \tag{71}$$

where $\psi(x)$ and $\phi(x)$ are given in Eqs. (42) and (44), respectively. Note that these eigenfunctions are normalized with respect to the mass distribution ρA. Hence, we obtain for the kinetic and potential energies

$$2T = \dot{\eta}^2(t) + \dot{z}^2(t) + M\dot{\eta}(t)\dot{z}(t)z(t), \quad 2V = \Omega_1^2\eta^2(t) + \varpi_1^2 z^2(t), \tag{72}$$

where from Eq. (35), $\varpi_1^2 = a_1^4/\rho A$ (transverse motion) and $\Omega_1^2 = b_1^2/\rho A$ (axial motion), we have

$$M = \int_0^1 \rho A\psi(x)\phi(x)\phi'(x)\,\mathrm{d}x. \tag{73}$$

Considering the form of the virtual work in Eq. (33), and invoking Lagrange's equations, we obtain the equations of motion as

$$\ddot{\eta}(t) + Mz(t)\ddot{z}(t) + M\dot{z}^2(t) + \Omega_1^2\eta(t) = N(t), \tag{74}$$

$$\ddot{z}(t) + Mz(t)\ddot{\eta}(t) + \omega_1^2 z(t) = Z(t), \tag{75}$$

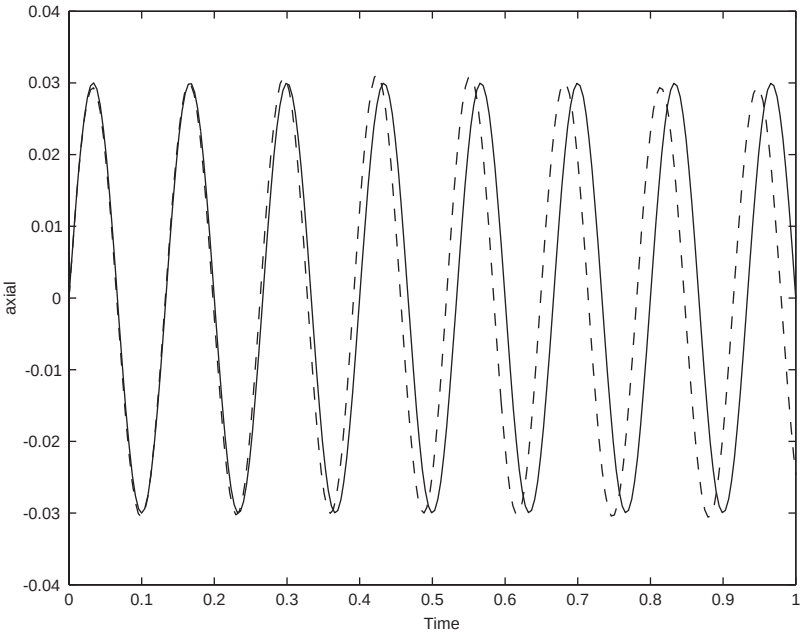

Fig. 13. Axial deformation: linear vs. non-linear model, - -, non-linear; —, linear.

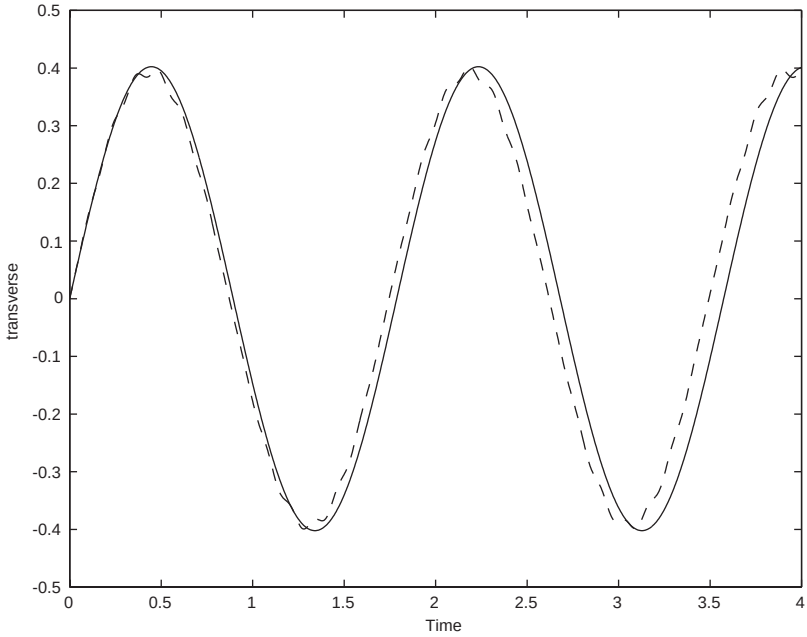

Fig. 14. Transverse deformation: linear vs. non-linear model, - -, non-linear; —, linear.

with N and Z denoting the generalized forces. We basically integrate these two equations of motion to obtain the response.

A numerical evaluation of M, for the parameters of $\rho A = 1$, $\kappa = 1/30$ yields $M = 0.7228$. With this information, zero initial conditions and an impulsive force applied at angle of 45° to the beam axis (same conditions as considered in previous examples) we integrate the equations of motion.

Plots of $\eta(t)$ (axial co-ordinate) and $z(t)$ (transverse co-ordinate) are shown in Figs. 13 and 14 for the non-linear model, as well as the linearized model. As can be seen, the primary effect of the non-linearity is a small change in the period of the motion, with no noticeable change in the vibration amplitudes. This is the type of plot one observes when studying a pendulum that undergoes large motions. The coupling between the axial and transverse motions also appears to have negligible effect. It should be noted that similar results were obtained for different values of ρA and κ. Hence, we conclude that non-linearities in the equations of motion have no discernible effect on vibration amplitudes and that our earlier results, which are based on the linearized model, are valid for the general system.

7. Conclusions

We compared for slender beams the amplitude ratios of the axial elastic deformation versus the shortening of the projection. We developed closed-form solutions for axial and transverse deformations for a fixed–free beam with an impulsive force at its free end. The results indicate that the shortening of the projection and elastic stretch have comparable magnitudes with the shortening of the projection being slightly larger in a majority of cases. When modelling a specific

beam, it is recommended that one first analyze the relative magnitudes of the shortening and axial elasticity using the amplitude ratios developed above as guidelines.

Appendix A. Closed-form solution for axial and transverse vibrations

In this appendix, we develop a closed-form solution for the response of a beam (in bending or axial vibration) with a free end. We consider that a force F_e is applied at the free end. Since there is a force at the free end, the free-end boundary conditions no longer apply. First, we consider the axial vibration, given by Eq. (21).

We can model the beam and the excitation applied to it in two ways: In the first way, we write the external excitation as

$$p_x(x,t) = F_e(t)\delta(x - L^-), \tag{A.1}$$

with the mathematical manipulation that the force is not really at the free end, but at an infinitesimal distance behind it. This makes it possible to use the standard model expansion, as outlined previously in the text.

The second and more mathematically sound way of dealing with the force in the free end is outlined in Refs. [5,6]. Here, we consider that procedure, as well as suggest an improvement. The boundary conditions are no longer homogeneous:

$$e(0,t) = 0, \quad EA\left.\frac{\partial e(x,t)}{\partial x}\right|_{x=L} = F_e(L,t). \tag{A.2}$$

For simplicity, we assume zero initial conditions. We will consider a solution in the form

$$e(x,t) = e_1(x,t) + h(x)F_e(L,t). \tag{A.3}$$

The function $h(x)$ can be chosen in many different ways; here we select $h(x)$ in the following form, so that $e_1(x,t)$ is the solution for fixed–free vibrating beam without any load at its free end:

$$h(x) = (a + bx)\bar{u}(x - L), \quad \frac{\mathrm{d}h(x)}{\mathrm{d}x} = a\bar{u}(x - L) + (a + bx)\delta(x - L), \tag{A.4}$$

and boundary conditions

$$h(x)|_{x=0} = 0, \quad \left.\frac{\mathrm{d}h(x)}{\mathrm{d}x}\right|_{x=0} = 0, \quad h(x)|_{x=L} = 0, \quad EA\left.\frac{\mathrm{d}h(x)}{\mathrm{d}x}\right|_{x=L} = 1, \tag{A.5}$$

where $\bar{u}$ is the step function and δ is the impulse function. The coefficients a and b are determined by using the initial conditions. This leads to

$$h(x) = \left(-\frac{L}{EA} + \frac{1}{EA}x\right)\bar{u}(x - L). \tag{A.6}$$

Introducing Eq. (A.3) into the equation of motion we obtain

$$-EA\frac{\partial^2 e_1(x,t)}{\partial x^2} + \mu(x)\frac{\partial^2 e_1(x,t)}{\partial t^2} = EA\frac{\mathrm{d}^2 h}{\mathrm{d}x^2}F_e(x,t) - \mu(x)h(x)\ddot{F}_e(x,t) \tag{A.7}$$

with homogeneous boundary conditions

$$e_1(x,t)|_{x=0} = 0, \quad EA\left.\frac{\partial e_1(x,t)}{\partial x}\right|_{x=L} = 0. \tag{A.8}$$

We assume a solution in the form $e_1 = U(x)T(t)$. After substituting this expression in the equation of motion we have

$$U_r(x) = \sqrt{\frac{2}{\mu L}}\sin(a_r x) = \sqrt{\frac{2}{\mu L}}\,\bar{U}_r(x), \tag{A.9}$$

where

$$a_r = (2r-1)\frac{\pi}{2L}, \quad \Omega_r = a_r\sqrt{\frac{EA}{\mu}}, \quad \bar{U}_r(x) = \sin(a_r x), \quad r = 1,2,\ldots. \tag{A.10}$$

The modal equations become

$$\ddot{\eta}_r(t) + \Omega_r^2\eta_r(t) = -\{N_r^* F_e(L,t) + N_r\ddot{F}_e(L,t)\}, \quad r = 1,2,\ldots \tag{A.11}$$

in which $\eta_r(t)$ are the modal co-ordinates and

$$N_r^* = \int_0^L U_r(x)\left(-EA\frac{\mathrm{d}^2 h}{\mathrm{d}x^2}\right)\mathrm{d}x = -U_r(L), \quad r = 1,2,\ldots, \tag{A.12}$$

$$N_r = \int_0^L \mu U_r(x)h(x)\,\mathrm{d}x = 0, \quad r = 1,2,\ldots. \tag{A.13}$$

For zero initial conditions the solution is

$$\eta_r(t) = \frac{1}{\omega_r}\int_0^t U_r(L)F_e(L,\tau-t)\sin(\Omega_r\tau)\,\mathrm{d}\tau, \quad r = 1,2,\ldots. \tag{A.14}$$

Up to this point we did not use the fact that the force is an impulsive force, so that the modal equations (A.14) are valid for any force acting at the free end. When the force at the end of the beam is an impulsive force, $F_e(L,t) = \hat{F}_e\delta(t)$, the modal equations become

$$\eta_r(t) = \frac{1}{\Omega_r}U_r(L)\hat{F}_e\sin(\Omega_r t) = \frac{1}{\Omega_r}\sqrt{\frac{2}{\mu L}}\,\bar{U}_r(x)\hat{F}_e\sin(\Omega_r t), \quad r = 1,2,\ldots \tag{A.15}$$

and the complete solution for the axial stretch is

$$e(x,t) = \sum_{r=1}^{\infty} U_r(x)\eta_r(t) + \left(-\frac{L}{EA} + \frac{1}{EA}x\right)\bar{u}(x-L)\hat{F}_e\delta(t). \tag{A.16}$$

This procedure can easily be extended to the transverse vibration of beams. The solution is in the form

$$v(x,t) = v_1(x,t) + h_v(x)F_v(x,t). \tag{A.17}$$

where one can show that

$$h_v(x) = \left(-\frac{L^3}{6EI} + \frac{L^2}{2EI}x - \frac{L}{2EI}x^2 + \frac{1}{6EI}x^3\right)\bar{u}(x-L), \tag{A.18}$$

$$h_v(x)|_{x=0} = 0, \quad \left.\frac{\mathrm{d}h_v(x)}{\mathrm{d}x}\right|_{x=0} = 0, \quad \left.\frac{\mathrm{d}^2h_v(x)}{\mathrm{d}x^2}\right|_{x=0} = 0, \quad \left.\frac{\mathrm{d}^3h_v(x)}{\mathrm{d}x^3}\right|_{x=0} = 0,$$

$$h_v(x)|_{x=L} = 0, \quad \left.\frac{\mathrm{d}h_v(x)}{\mathrm{d}x}\right|_{x=L} = 0, \quad \left.\frac{\mathrm{d}^2h_v(x)}{\mathrm{d}x^2}\right|_{x=L} = 0, \quad EI\left.\frac{\mathrm{d}^3h_v(x)}{\mathrm{d}x^3}\right|_{x=L} = 1, \tag{A.19}$$

and $v_1(x,t)$ is the solution for

$$EI\frac{\partial^4 v_1(x,t)}{\partial x^4} + \mu(x)\frac{\partial^2 v_1(x,t)}{\partial t^2} = -\left\{EI\frac{\mathrm{d}^4 h_v}{\mathrm{d}x^4}F_v(L,t) + \mu(x)h_v(x)\,\ddot{F}_v(L,t)\right\}, \tag{A.20}$$

with zero initial conditions and the boundary conditions

$$v_1(0,t) = 0, \quad \left.\frac{\partial v_1(x,t)}{\partial x}\right|_{x=0} = 0, \quad \left.\frac{\partial^2 v_1(x,t)}{\partial x^2}\right|_{x=L} = 0, \quad EI\left.\frac{\partial^3 v_1(x,t)}{\partial x^3}\right|_{x=L} = 0. \tag{A.21}$$

The solution can then be expressed as $v_1(x,t) = \sum_{r=1}^{\infty} V_r(x)\eta_r(t)$:

$$V_r(x) = \sqrt{\frac{1}{\mu L}}\frac{1}{\sqrt{I_r}}\{\cosh(b_r x) - \cos(b_r x) - \sigma_r(\sinh(b_r x) - \sin(b_r x))\}, \quad r = 1,2,\ldots, \tag{A.22}$$

$$b_1 L = 1.875, \quad b_2 L = 4.694, \quad b_3 L = 7.855, \quad b_4 L = 10.996, \tag{A.23}$$

$$\sigma_r = \frac{\cos(b_r x) + \cosh(b_r x)}{\sin(b_r x) + \sinh(b_r x)}, \quad \omega_r^2 = b_r^4\frac{EI}{\mu}, \quad r = 1,2,\ldots,$$

$$I_r = \frac{1}{L}\int_0^L \{\cosh(b_r x) - \cos(b_r x) - \sigma_r(\sinh(b_r x) - \sin(b_r x))\}^2\,\mathrm{d}x, \tag{A.24}$$

$$\eta_r(t) = \frac{1}{\omega_r}\int_0^t V_r(L)F_v(L,\tau - t)\sin(\omega_r\tau)\,\mathrm{d}\tau, \quad r = 1,2,\ldots. \tag{A.25}$$

When the force at the end of the beam is an impulsive force $F_v(L,t) = \hat{F}_v\delta(t)$, the solution is

$$\eta_r(t) = \frac{1}{\omega_r}V_r(L)\hat{F}_v\sin(\omega_r t) = \frac{1}{\omega_r}\sqrt{\frac{1}{\mu L}}\,\bar{V}_r(x)\hat{F}_v\sin(\omega_r t), \quad r = 1,2,\ldots, \tag{A.26}$$

and the complete solution for transverse vibration becomes

$$v(x,t) = \sum_{r=1}^{\infty} V_r(x)\eta_r(t) + \left(-\frac{L^3}{6EI} + \frac{L^2}{2EI}x - \frac{L}{2EI}x^2 + \frac{1}{6EI}x^3\right)\bar{u}(x-L)\hat{F}_v\delta(t). \tag{A.27}$$

Using the above expression the shortening of the projection at the tip of the beam is

$$S(L,t) = -\frac{1}{2}\frac{1}{(\mu L)^2}\int_0^L \left(\sum_{r=1}^{\infty}\frac{\mathrm{d}\bar{V}_r(x)}{\mathrm{d}x}\frac{1}{\omega_r}\bar{V}_r(L)\hat{F}_v\sin(\omega_r t)\right) \times \left(\sum_{s=1}^{\infty}\frac{\mathrm{d}\bar{V}_s(x)}{\mathrm{d}x}\frac{1}{\omega_s}\bar{V}_s(L)\hat{F}_s\sin(\omega_s t)\right)\mathrm{d}x, \tag{A.28}$$

where we used the fact that $h(x) = 0$, $\mathrm{d}h(x)/\mathrm{d}x = 0$ for $0 \leqslant x \leqslant L$.

The difference between the response obtained here ($v(x,t)$) and the response obtained using a straightforward expansion (which is the same as $v_1(x,t)$) is in the third and fourth derivatives, namely in the shear and moment expressions. While the free end approach gives the erroneous result of zero shear force, the developments in Refs. [5,6] and the solution above shows that shear force is not zero at that point.

References

[1] H. Baruh, *Analytical Dynamics*, McGraw-Hill, New York, 1998.
[2] I. Sharf, A survey of geometric stiffening in multibody dynamics formulations, in: A. Guran, D.J. Inman (Eds.), *Wave Motion, Intelligent Structures and Nonlinear Mechanics*, Series on Stability, Vibration and Control of Structures, Vol. 1, World Scientific, Singapore, 1995.
[3] R.A. Laskin, P.W. Likins, R.W. Longman, Dynamical equations of a free–free beam subjected to large overall motions, *Journal of Astronautical Sciences* 31 (1983) 507–528.
[4] S.M. Han, H. Benaroya, T. Wei, Dynamics of transversely vibrating beams using four engineering theories, *Journal of Sound and Vibration* 225 (5) (1999) 935–988.
[5] H. Benaroya, *Mechanical Vibration*, Prentice-Hall, Englewood Cliffs, NJ, 1997.
[6] L. Meirovitch, *Principles and Techniques of Vibrations*, Prentice-Hall, Englewood Cliffs, NJ, 1998.